INFLUENCE OF ALUMINIUM DOPING ON RANDOM LASING IN ZnO NANORODS

NUR FADZLIANA BINTI RAMLI

UNIVERSITI SAINS MALAYSIA

2020

INFLUENCE OF ALUMINIUM DOPING ON RANDOM LASING IN ZNO NANORODS

by

NUR FADZLIANA BINTI RAMLI

Thesis submitted in fulfilment of the requirements
for the degree of
Master of Science

October 2020

ACKNOWLEDGEMENT

In the name of Allah, the Most Gracious and the Most Merciful. All praises to Allah for His blessing and strength given to me on completing this research and thesis. First of all, I would like to express my highest gratitude to my lovely supervisor Dr. Wan Maryam Wan Ahmad Kamil for her long and endless support, guidance, and hear-warming attitude toward my efforts over the course of completing this journey which a lot of things happened. I am also thankful to my co-supervisor Dr. Siti Azrah Mohamad Samsuri for all the guidance and input she has made to the direction of this research.

I would also like to express my sincere gratitude to the Assoc. Prof Dr Hsu Cheng Hsu and his student from the Department of Photonics, National Cheng Kung Taiwan for the collaboration opportunity to observe random lasing in our samples. My acknowledgment also goes to all staff of INOR lab for guidance in using the required equipment and material related to my works. Also, to the team members of random lasing group, thank you for all the supports.

I also would like to take this opportunity to thank the Universiti Sains Malaysia for providing the platform to pursue this study and financial support through bridging grant: 304.PFIZIK.6316077 and FRGS grant: 203.PFIZIK.6711667. Not to forget, I acknowledge my indebtedness gratitude to my parents and family for their continued faith, encouragement and pray for the success of this journey and my life. Finally, I would like to thanks all my friends and any person who contributed to my research directly or indirectly.

TABLE OF CONTENTS

LIST OF TABLES

LIST OF FIGURES

LIST OF SYMBOLS

Å	Angstrom, 10^{-10} m
Atm	Atmosphere
a.u	Arbitrary unit
C	Lattice parameter of miller indices
^{o}C	Celcius
D	Interplanar spacing in the crystalline material
D	Average crystallite size
eV	Electron volt
H	Hour
Hz	Hertz
K	Constant with value 0.9
KHz	Kilo hertz
L	Laser cavity length
N	Integer
Nm	Nanometer, 10^{-9} m
meV	Mili electron volt, 10^{-3} eV
Ml	Millilitre
Min	Minutes
mW	Milliwatts
mA	Milli ampere
Mbar	Milli bar
μm^2	Micrometer square
mJ/cm^2	Milli joule per square centimetre
θ	Diffraction angle

μ	Micro, 10^{-6}
λ	Wavelength
ε	Strain
W	Watt

LIST OF ABBREVIATIONS

Al	Aluminium
ASE	Amplified spontaneous emission
Avg.	Average
CBD	Chemical bath deposition
CVD	Chemical vapor deposition
CO_2	Carbon dioxide
Cu	Copper
Cu-Kα	Copper K (alpha)
DLE	Deep level emission
FESEM	Field emission scanning electron microscopy
FWHM	Full width half maxima
GaN	Galium nitrate
H_2	Hydrogen gas
HMT	Hexamethylenetetramine
ITO	Indium tin oxide
LASER	Light amplification by stimulated emission of radiation
MBE	Molecular beam epitaxy
MOCVD	Metal-organic chemical vapour deposition
MOVPE	Metal-organic vapour-phase epitaxy
NBE	Near band edge
NIR	Near infrared
N_2	Nitrogen gas
Nd:YAG	Neodymium-doped yttrium aluminium garnet
O_2	Oxygen

PLD	Pulse laser deposition
PL	Photoluminescence
PVD	Physical vapour deposition
RF	Radio frequency
RT	Room temperature
RL	Random laser
SEM	Scanning electron microscopy
VLS	Vapour liquid solid
XRD	X-ray diffraction
ZnO	Zinc oxide
1D	One dimensional
μ-PL	Micro-photoluminescence

PENGARUH ALUMINIUM TERHADAP LASER RAWAK DI DALAM ZNO NANOROD

ABSTRAK

Tujuan kajian ini dijalankan adalah untuk mengkaji ciri struktur, optik dan pancaran laser rawak daripada aluminium (Al) didopkan pada ZnO nanorod dihasilkan di atas gelas yang diseliputi indium tin oksida (ITO) melalui kaedah pemendapan rendaman kimia (CBD). Perbezaan kepekatan aluminium digunakan iaitu 0 (ZNO), 0.25 (AZ1), 5 (AZ2), 10 (AZ3), 30 (AZ4), dan 50 (AZ5) mM untuk dikaji. Majoriti nanorods menunjukkan struktur tirus dan lompang antara nanorods lebih ketara dengan peningkatan kepekatan Al. Perbezaan dop kepekatan menunjukkan perbezaan purata diameter nanorod berbeza antara 29.22 nm dan 33.80 nm. Pembentukan fasa ZnO wurtzite dengan (002) sebagai orientasi keutamaan telah disahkan menggunakan analisis pembelauan X-ray. Keserapan spektrum untuk semua sampel kecuali sampel AZ5 menunjukkan sifat penyerapan yang baik di bawah 400 nm UV. Di samping itu, kedua-dua tidak didopkan dan Al didopkan nanorod menunjukkan nilai yang tinggi lutsinar diantara 85% ke 70% pada julat UV-kelihatan. Analisis lanjut menunjukkan nilai jurang optik meningkat dari 3.209 eV (tidak didop) kepada 3.27 eV (AZ3) apabila kepekatan dop meningkat. Spektrum fotoluminesen menunjukkan pelepasan UV yang kuat pada kira-kira 400 nm untuk pelepasan pinggir berhampiran (NBE) ZnO dan puncak pelepasan yang dapat dilihat dari titik kecacatan di dalam sampel. Akhirnya, laser rawak disiasat oleh spektroskopi mikro-PL. Dua mod di dalam sampel tidak didop berkurang kepada satu mode di dalam sampel yang didop. Ambangan laser menurun pada mulanya dari 4490 μW (tidak didop) kepada 5.5 μW (AZ3). Walaubagaimanapun, meningkat

kepekatan seterunya meningkatkan ambangan. Ambang yang dikurangkan dalam pelepasan yang dilepaskan adalah sekurang-kurangnya 2 magnitud diperhatikan dalam sampel dop berbanding dengan ZnO munkin disebabkan pemindahan tenaga oleh Al meningkatkan laser rawak. Ambang terendah diperolehi daripada AZ3, menunjukkan kepekatan dop terbaik adalah 10 mM. Keputusan menunjukkan kemungkinan mengendalikan sifat laser rawak adalah dengan menyesuaikan kepekatan dop. Ini berguna untuk menghasilkan laser rawak yang cekap dalam masa terdekat.

INFLUENCE OF ALUMINIUM DOPING ON RANDOM LASING IN ZNO NANORODS

ABSTRACT

The purpose of this study is to investigate the structural, optical and random lasing characteristics from aluminium (Al) doped ZnO nanorods fabricated on ITO coated glass substrates using chemical bath deposition (CBD) technique. Different Al doping concentration 0 (ZnO), 0.25 (AZ1), 5 (AZ2), 10 (AZ3), 30 (AZ4) and 50 (AZ5) mM were explored. The majority of nanorods show a tapered structure with at the tip and voids between nanorods were more apparent with increasing Al concentration. Different doping concentration shows different average nanorod diameter between 29.22 nm and 33.80 nm. The formation of wurtzite ZnO phase with (002) as preferential orientation was confirmed by X-ray diffraction analysis. The absorbance spectra for all sample except sample AZ5 exhibited good UV absorption properties below 400 nm. In addition, both undoped and Al-doped nanorod exhibit high transparency approximately 85% to 70% in the UV-Visible range. Further analysis showed increase in optical bandgap from 3.209 eV (undoped) to 3.274 eV (AZ4) when doping concentration increases. Photoluminescence spectra showed a strong UV emission at about 400 nm for the near band edge (NBE) emission of ZnO and visible emission peak from point defects. Finally, random lasing was investigated. The double mode in undoped sample is reduce to single mode in doped sample. The lasing threshold decrease at first from 4490 μW (undoped) to 5.5 μW (AZ3). However, increasing the concentration further increase the threshold. Thereshold was 2 orders of magnitude lower than undoped ZnO possibly due to the aluminium embedded in the ZnO nanorod. Lowest threshold was

obtained from AZ3; suggesting best doping concentration is 10 mM. Results indicated the possibility of controlling random lasing properties by adjusting the doping concentration. This would be useful in developing efficient random lasers in the near future.

CHAPTER 1

INTRODUCTION

1.1 Introduction

This chapter discusses the fundamental properties of ZnO and literature readings of incorporating its structure. Following this, the different methods of synthesizing ZnO will be elaborated with an emphasis on the chemical bath deposition (CBD) method. Next, current studies on doping ZnO that are related to this work will be discussed in detail. This is followed by explaining the concept of lasing and random lasing, including random laser applications. In the next section of this chapter, the problem statement and research gap, research objective, and research scope are addressed. Finally, the outline of this thesis will be presented.

1.2 Fundamentals of ZnO

Zinc Oxide (ZnO) is a popular semiconducting material since the 1930s [1]. In the last 20 years, ZnO has experience interest in scientific research due to its great versatility in terms of synthesis methods for epitaxial layers and it is widely used in various industrial products as summarized in Figure 1.1 [2]. Now, the new area for ZnO started in the field of photonics and optoelectronic by the impressive progress in developing efficient short-wavelength emitters based on wide band-gap semiconductors [3]. Many techniques, both physical and chemical have been employed in advancing ZnO structures.

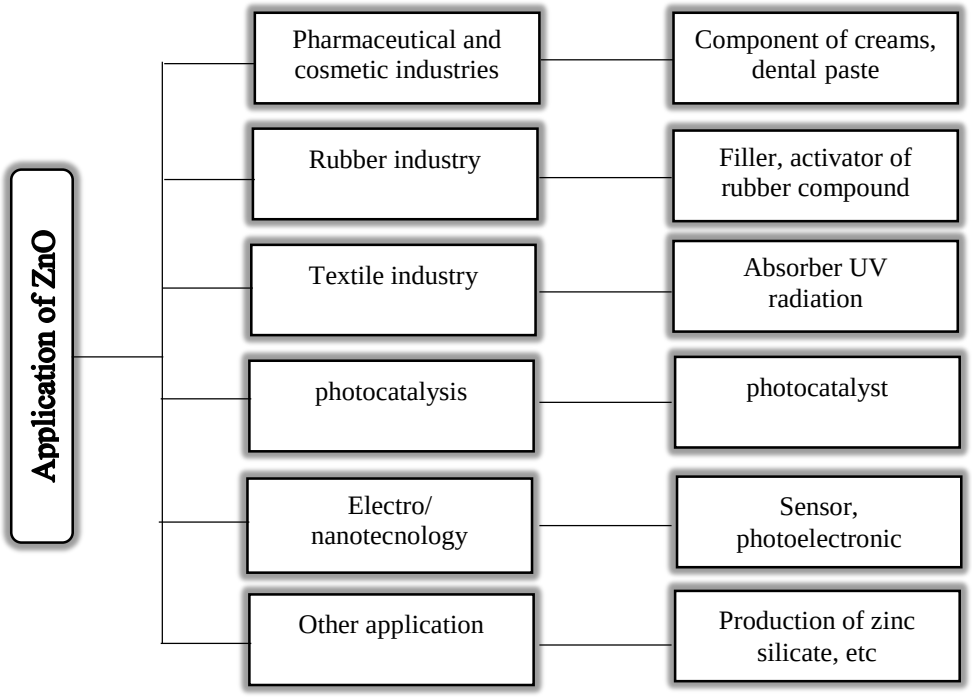

Figure 1.1 Industrial applications of ZnO

One of the most interesting aspects of ZnO is the possibility to easily grow in different nanoscale form. Figure 1.2 (a-d) reports a collection of ZnO nanostructure with different techniques of growth: nanobelt (NBs) [4], aligned nanorods (NWs) [5], nanotube (NTs) [6], and nano propellers [7]. Current research has been focused on these nano and micro-scale structures, representing the fundamental building blocks of modern physics and engineering. Nanowires are ideal for studying one dimensional transport, especially in understanding key fundamental concepts in low dimensional systems and generating nanodevices. The basic material parameters of ZnO are shown in Table 1.1 [8].

Table 1.1 Basic physical parameters of ZnO lattice at 300 K [8].

Physical parameter	Value
Lattice constant, a	0.32495 nm
Lattice constant, c	0.52069 nm
Ratio a/c	1.602 (ideal hexagonal structure shows 1.633)
Density	5.606 g/cm^3
Stable phase at 300 K	Wurtzite
Melting point	1975 °C
Thermal conductivity	60.0 W/m-K
Linear expansion coefficient	a: 6.5 ×10^{-6} -°C
	c: 3.0 × 10^{-6} -°C
Static dielectric constant, ε	8.12 x (8.8542 x 10^{-12}) (Fm^{-1})
Refractive index	2.008, 2.029
Energy gap	3.37 eV, direct
Intrinsic carrier concentration	<10^6 cm^{-3} (max n-type doping>10^{20} cm^{-3} electrons; max p-type doping<10^{17} cm^{-3} holes)
Exciton binding energy	60 meV
Electron effective mass	9.11 x 10^{-31} kg
Electron Electron Hall mobility at 300 K for low n-type conductivity	200 cm^2/V s
Hole effective mass	9.11 x 10^{-31} kg
Hole Hall mobility at 300 K for low p-type conductivity	5–50 cm^2/V s

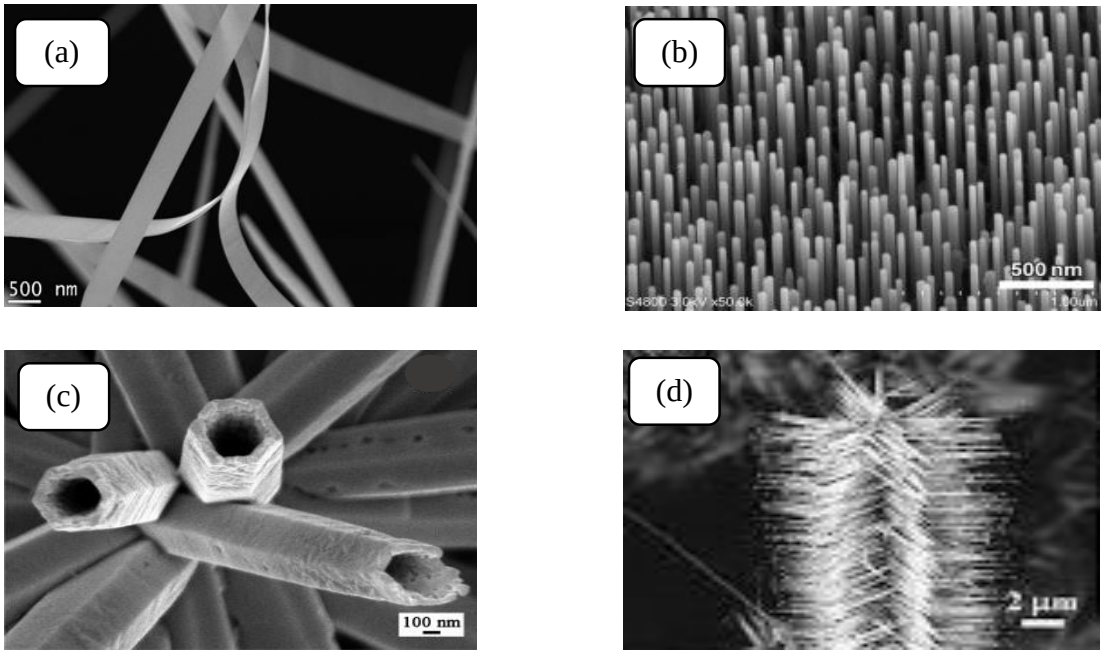

Figure 1.2 Collection of ZnO structure: (a) nanobelt [4], (b) aliged nanowire arrays/nanorods [5], (c) nanotube [6] and (d) array of propellers [7].

1.3 Problem Statement

Nowadays, the products of the semiconductor industry spread all over the world and deeply penetrate our daily life. Silicon has been dominating the commercial market for making discrete device and integrated circuits for computing, data storage as well as communication devices. Since Si has indirect bandgap which is not suitable for the optoelectronic device, GaAs with direct bandgap stand out and fills the blank. However one of the biggest challenges with this material is the requirement of ultraviolet (UV)/blue light emitter application which is beyond the limits of GaAs. Therefore, the wide bandgap GaN and ZnO nanostructures turn into research focus in the field of a semiconductor.

ZnO nanostructure has long been successfully synthesized through various different methods such as MOCVD [9], molecular beam epitaxy (MBE) [10], laser ablation [11] and sputtering [12] technique. However, these methods are complex processes, sophisticated equipment, and high temperatures make them very hard to large scale production for commercial applications. On the contrary, hydrothermal methods like the CBD technique requires low operating temperatures, minimal lab equipment and versatility in managing growth. However, precision of size control and reproducibility is poor. This is especially so when the lattice mismatch of the substrate with ZnO is high. Up to our knowledge, the best way to minimize these problems is by introducing a seed layer prior to growth. To reduce defects on lattice site, annealing may also be introduced before and/or after CBD. Up to date, reports on Al-doped ZnO nanowires synthesis particularly via the method we have adopted are scarce. Therefore, the focus here is to synthesize aluminium doped zinc oxide nanorod by two step CBD and understand its influence on the structural and optical properties of ZnO:Al.

Furthermore, the major problem is to have a better understanding of random lasing behaviour when doping is done through CBD. Optically pumped random lasing on ZnO nanostructure has been successfully created by previous research and the concept of it is well established. Doping in a semiconductor has been utilized in a number of laser systems, especially in achieving low injection currents in electrically pumped lasers. However, it has also been used to achieve lasing and improve lasing performance in some laser systems. In particular, the synthesis of aluminium doped zinc oxide nanorods by using CBD has not been attempted random lasing. Hence, this work seeks to explore the effect of aluminium doped zinc oxide on random lasing properties. It has also been highlighted that some form of defects plays a role in controlling random lasing emission. So, the doping act as point defects in the sample and the role of Al in controlling random lasers will be investigated.

1.4 Research Objective

1. To synthesize Al doped ZnO nanorod with different concentrations of Al using a chemical bath deposition technique.

2. To identify the morphology, crystal structure, crystalline quality and optical properties of the Al doped ZnO nanorods.

3. To determine the random lasing threshold and the number of lasing modes in Al doped ZnO nanorods.

1.5 Scope of Study

This thesis focuses on the effect of Al concentration in ZnO nanorods on ITO glass substrate prepared by two-step chemical bath deposition technique. More specifically, the different concentrations of Al are introduced in zinc oxide nanorod to investigate the effect on random lasing behaviour.

The emphasis here will be to synthesize and characterize the structural properties of Al doped ZnO with dopant concentrations ranging from 0 mM to 50 mM. All the samples are characterized by FESEM, EDX, UV-Vis, PL to obtain nanorod morphology, orientation, crystal structure, and optical properties.

The work then focuses on the establishment of random lasing from the sample by micro-PL. This measurement provides information on the lasing threshold condition, the number of lasing modes and its wavelength, linewidth, and lasing intensity.

1.6 Thesis Outline

This thesis is divided into six chapters as follows:

Chapter 1 The problem statements, research gap, research objective, scope of study and thesis outline are included and discussed.

Chapter 2 gives detail about the theoretical concept in relation to this study. A brief concept of formation of thin film, the concept of doping, and the theoretical part of photoluminescence and random lasing will be discussed, including their related literature reviews.

Chapter 3 describes the methodology and instrument. The first part of this chapter will deal with the preparation of samples from the cleaning process to the growth of nanorods and ends with annealing treatment. The second part is the characterization technique used to study the characteristic of nanorods including morphology, orientation, crystallinity, optical properties, and random lasing.

Chapter 4 focuses on the result and discussion analysis of the morphology and structure of nanorods provided by FESEM, crystallinity and element of the nanostructure information from XRD, and information on optical properties obtained from the UV-Vis and photoluminescence (PL).

Chapter 5 focuses on the result and discussion of random lasing behaviour on doped and undoped ZnO nanorods. Discussion includes lasing threshold, linewidth, intensity and wavelength of random lasing emission.

Chapter 6 gives a summary of the key results and conclusion from this

work. Recommendation for future work is also included.

CHAPTER 2

THEORETICAL CONCEPT AND LITERATURE REVIEW

2.0 Introduction

This chapter explains the classification and the theoretical concept regarding synthesis of nanomaterial followed by the concept of the formation of the thin film. The basic principle of the CBD technique will also be elaborated. The concept of doping in ZnO, photoluminescence and random laser are also discussed.

2.1 Classification and Synthesis of Nanomaterials

To date, the idealization of semiconductor structures which includes quantum wells, wires, and dots have gained lots of attention due to the ability to synthesize various surface morphologies and structures of the semiconductor materials within near-atomic scale. Quantum mechanics are used to describe the different density of states for the electrons in these structures. The nanocrystals can be classified into zero-dimension (0-D), one-dimension (1-D), two-dimension (2-D) and three-dimension (3-D). 0-D nanostructures represent quantum dots or nanoparticles, 1-D nanostructures are commonly ascribed to nanowires, nanorods, nanofibres, nanobelts, and nanotubes, 2-D nanomaterials refer to nanosheets, nanowalls, and nanoplates and 3-D nanomaterials are nanoflowers and other complex structures [13]. Depending on the degree of confinement, the density of states is remarkably changed for different types of nanostructures. The classifications of different forms of nanostructure are illustrated in Figure 2.1 [14].

Nanomaterials have an extremely small size which has at least one dimension 100 nm or less. The method to synthesis nanomaterials is divided into two groups which are ‘bottom-up’ and ‘top-down’ approaches. The bottom-up approaches are methods that build nanomaterials from atomic or molecular precursors while top-down approaches involve tearing down a larger scale of building blocks into finer pieces until the nanoscale level is reached. The schematic diagram of these two approaches is presented in Figure 2.2 [14].

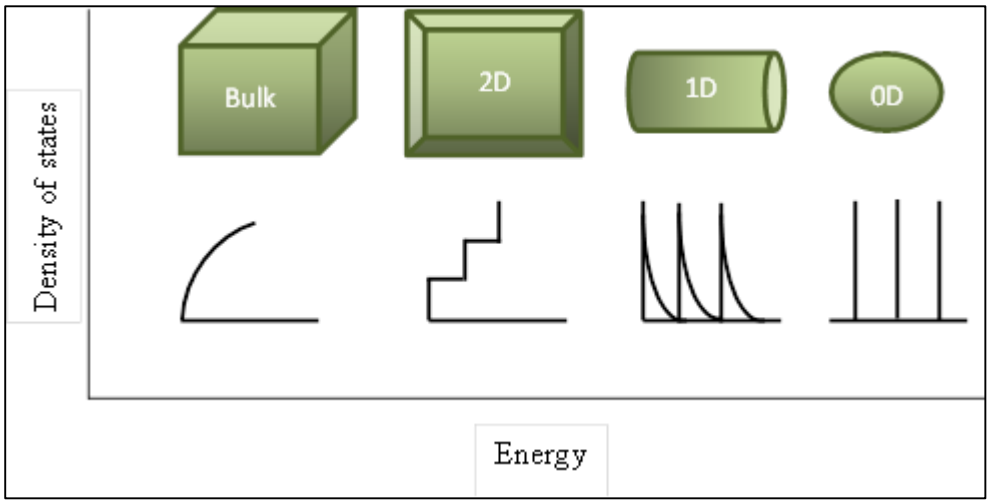

Figure 2.1 Schematic representation of (a) 0- dimension (0-D), (b) 1-dimension (1-D), (c) 2- dimension (2-D) and 3- dimension (3-D) systems with their coresponding density of state [14].

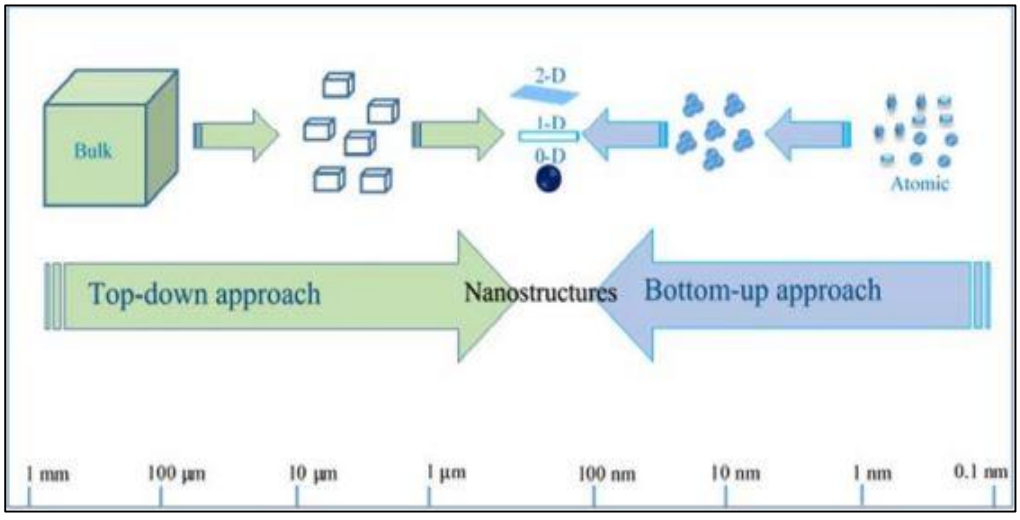

Figure 2.2 Top-down and bottom-up approaches to synthesis nanomaterials [14].

2.2 Formation of Thin Film

In brief, a low dimensional material made up by deposition of elements (metal, semiconductor, insulator, dielectric) atom by atom on a substrate through a phase transformation can be classified as thin film. The vital processes to form thin-film include condensation, nucleation, and growth. Figure 2.3 is a schematic illustration showing the major atomic processes: (a) deposition of atoms from the vapor onto the substrate surface or existing clusters; (b) diffusion of adatoms on the surface; (c) nucleation of adatom clusters; (d) addition of mobile adatoms to the existing clusters; (e) dissociation of clusters, and (f) a dynamic equilibrium is reached when the evaporation of the absorbed atoms from substrate surface and the deposition of the atoms from the vapor occur simultaneously [15].

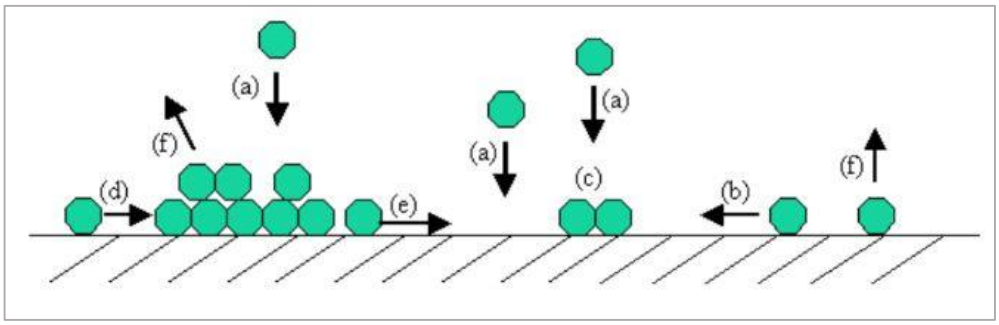

Figure 2.3 A Schematic illustration of thin-film growth steps: (a) Deposition of atoms from the vapor (b) Surface movement/ diffusion of the adatoms (c) Formation of clusters by nucleation (d) Addition of adatoms to existing clusters (e) Dissociation of a cluster and (f) Evaporation [15].

2.2.1 Condensation

Condensation means the transformation of a gas into a liquid or solid. Condensation of a vapour atom is determined by its interection with the surface of the substrate when the partial vapour pressure is equal or greater than its vapour gas state at room temperature. The impinging atom is attracted to the surface by the instantaneous dipole and quadrupole moment of the surface atoms. If the substrate material is different from the vapour material, the impinging atoms are first adsorbed (called ad atom) on the surface of the substrate but it may or may not be completely thermal equilibrated. It may move over the surface by jumping from one potential to the other because of the thermal activation from the surface and its own kinetic energy parallel to the surface. The ad atom may interact with the other ad atom to form a stable cluster by chemically adsorbed with release the heat of condensation. These small clusters then act as the initial centers of condensation.

2.2.2 Nucleation

The formation of thin film starts with nucleation. As absorbed atoms combine, they form a small cluster (nuclei) and produce condensation. The formation process is referred as the nucleation stage. Nucleation can be separated into two; 1) Homogeneous, in the absence of foreign particles or crystals in the solution or 2) Heterogeneous, in the presence of foreign particles in the solution. Homogenous and heterogenous nucleation stage are considered as the primary nucleation. A secondary nucleation occurs when crystals from the same substance is present.

2.2.3 Growth

Crystal growth occurs by increasing the size of the crystal through impingement of an atom or molecule at the surface. There are four stages of growth process based on the electron microscope observation as illustrated in figure 2.4:

1) The island stage

2) Nucleation growth stage

3) The coalescence stage

4) The continuous film stage

When a substrate under the impingement of condenses monomers is observed in the electron microscope, these indicate that the condensation is a sudden burst of nuclei. These larger nuclei are three dimensional in nature with their height much less than their lateral dimensions. These larger nuclei appear as islands onto the substrate with a lot of unoccupied space between them and hence this stage is called the island stage.

Further, into the process of thin-film growth, the islands are combined with the neighboring ones to form larger islands. The phenomenon of the formation of larger islands from the smaller ones is called agglomeration or coalescence. This coalescence stage involves the transfer of mass between islands by diffusion and hence small islands disappear rapidly. The time of coalescence is very short, of the order of about 0.6 seconds.

As a consequence of the arrival of more and more species on the substrate, the coalescence continues, resulting in a network of the deposited areas with

channels (void spaces) in between. These channels last only for a small time, as some secondary nuclei begin to grow within these void spaces. It is the final stage of the thin film growth. This process is slow and filling the empty channels which required a considerable amount of deposits. Further deposition of the material leads to the diminishing or even vanishing of these voids resulting in an eventually continuous film, even though some pores may be present in some cases.

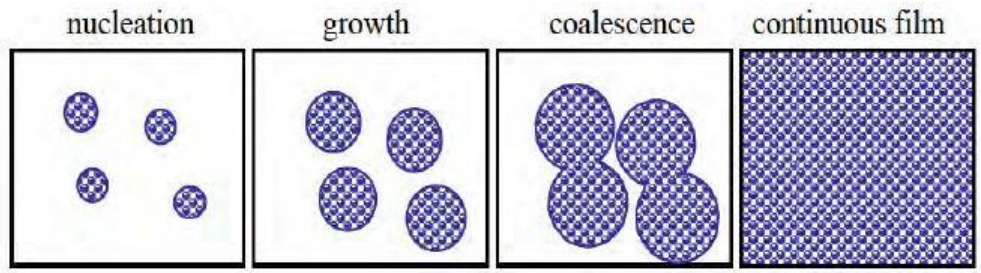

Figure 2.4 Different stage of thin-film growth.

2.3 The Basic Principle of CBD

Typically the thin film formation for CBD technique occurs in three steps: 1) creation of atomic/ molecular/ ionic species, 2) transport of these species through a medium and 3) condensation of these species. The CBD works on the principle of the controlled precipitation of the desired compound from a solution of its constituents. The precipitation is observed in a solution only when the ionic product exceeds the solubility product. The concept of the ionic product and solubility product are described below [16].

The soluble salt AB was kept in water, a saturated solution containing A^+ and B^+ ions in contact with undissolved solid AB is obtained and equilibrium is obtained between the solid phase and ions in the solution as,

$$AB(S) = A^+ + B^- \tag{2.1}$$

According to the law of mass action in equilibrium condition,

$$K = \frac{C_A^+ C_B^-}{C_{AB}(S)} \tag{2.2}$$

where, C_{A^+}, C_{B^-} and C_{AB} are the concentrations of A^+, B^- and AB ions in the solution.

The concentration of a pure solid phase is a constant number

$$C_{AB}(S) = \text{Costant} = K'$$

$$K = \frac{C_A^+ C_B^-}{K'} \tag{2.3}$$

$$KK' = C_A^+ C_B^- \tag{2.4}$$

Since K and K' is a constant, the product of KK' is also constant, know as K_S, therefore the equation (2.4) becomes,

$$K_S = C_A^+ C_B^- \qquad 2.5$$

K_S is called solubility product (SP) and $(C_A^+ . C_B^-)$ is called the ionic product (IP). In the saturated condition of the solution, the ionic product of ions is equal to the solubility product. But when IP exceeds the SP, for example, IP/SP = S > 1, the solution is supersaturated, precipitation occurs and ions combine on the substrate and in the solution to form nuclei.

Standard CBD method employs immersion of the substrate in a chemical solution containing the chalcogenide source, the metal ions and base. A complexing agent is added to control the hydrolysis of the metal ion. The chalcogenide ions is released slowly into free metal ion concentration, making the solution more alkaline.

2.3.1 Mechanism of Growth for Al-doped ZnO Nanorods by CBD

Compare to all methods, CBD is the simplest method because the only requirement is the aqueous solution and can be done at a relatively low temperature. In CBD process, the structural properties of ZnO nanorods are strongly dependent upon both the morphology of the polycrystalline ZnO seed layer most commonly deposited by sol-gel or sputtering process and the growth conditions used in aqueous solution (the acidity or basicity of the reaction system, precursors, solvents, time and temperature).

In the present CBD process, the chemical precursors doping of ZnO nanorods can be simultaneously tuned by adding aluminum nitrate in the standard chemical system using zinc nitrate and hexamethylenetetramine (HMTA) in aqueous solution. The set of chemical reactions has been established to be the following equation formula [17]–[20].

$$(CH_2)_6N_4 + 6H_2O \rightarrow 6HCHO + 4NH_3 \quad 2.6$$

$$NH_3 + H_2O \leftrightarrow NH_4^+ + OH^- \quad 2.7$$

$$Zn(NO_3)_2 \rightarrow Zn^{2+} + 2NO_3^- \quad 2.8$$

$$Zn^{2+} + 2HO^- \leftrightarrow ZnO(s) + H_2O \quad 2.9$$

$$Al(NO_3)_3 \rightarrow Al^{3+} + 3NO_3^- \quad 2.10$$

$$2Al^{3+} + 6HO^- \leftrightarrow Al_2O_3 + 3H_2O \quad 2.11$$

Mixing hexamethylenetetramine (HMTA) with zinc nitrate hexahydrate generates a homogenous aqueous solution that contains ammonia (NH_3) and formaldehyde

(HCHO) species (reaction 2.6). When adding $Zn(NO_3)_2$ to Zn^{2+} ion, HMTA acts as a weak base buffer by providing OH^- ion to Zn^{2+} ion to form stable $Zn(OH)_2$ ion complexes that keeps the pH constant. This induces more surface defects due to increased H^+ ions, which attracts more O^{2-} ions at the surface. Finally, ZnO NRs are synthesized (reaction 2.9). $Al(NO_3)_3.9H_2O$ precursor is added to the reaction medium to generate Al^{3+} (reaction 2.10) in making Al doped ZnO nanorods (reaction 2.11).

2.4 Doping of ZnO

Practical applications in semiconductors demand changes in electrical, optical and magnetic properties during operation. This can be achieved through doping whereby impurities are introduced in small amounts. Doping changes the bandgap, hence varying the doping provide means of bandgap engineering. ZnO has the added advantage of providing UV lasing at room temperature and has been a material of choice in UV lasing. Dopants (impurities) may either have one additional or one less valence electron than the host. When the dopant has extra valence electron, they donate this electron to the lattice and contributes to the density of free electrons. As such, they create n-type semiconductors.Analogously, dopants with one electron valance less than the host atom are called acceptors as they take up an electron from the host atom and create positively charged holes. As such, p-type semiconductors are formed.

2.5 Photoluminescence

Luminescence is an electromagnetic (EM) radiation phenomenon due to excessive thermal radiation or light in the physical system. In semiconductors, when the energy of the incident photon is equal or more than the energy bandgap, it will excite the electron from the valence band into the conduction band. Radiative (photon emission) and non-radiative (phonon emission) processes may occur when these electrons return to the ground states. Upon optical excitation, the spontaneous emission of light is termed as photoluminescence. Based on photoluminescence data, impurities defect level, bandgap determination, recombination mechanism, and surface structure and excited states can be obtained.

The luminescence process can be divided into three: 1) excitement, 2) heat balance and 3) recombination [21]. Before light radiates onto a semiconductor nanostructure sample, the electron exists at valance band edge as shown in figure 2.5(a). During photoluminescence, light with energy illuminates the sample. This causes the semiconductor to absorb a photon, as shown in Figure 2.5(b). The incident photon energy, E_{blue}, is transferred to an electron, causing it to move from the valence energy level to a conduction energy level and leaves behind a hole in the valence band. During this process, electron-hole pairs are created. The heat balance or thermalization process occurs when excited pairs relax towards quasi-thermal equilibrium distribution and it loses some of its kinetic energy as it collides with the semiconductor lattice creating phonons. In each collision, it loses a discrete amount of energy (represented by the staircase in Figure 2.5(b-c)). The electron rapidly settles at the lowest vacant energy level, E_1, in this case. Further, the electron recombines with a hole and radiates light with energy equal to the difference between the energy levels in the conduction and valence band, E_{red} as shown in

figure 2.5(c). In this process is called radiative recombination, and for photoluminescence experiments, a detector measures the energy, via the frequency of light emitted from this process. Finally, the electron is left in the valence band level as before (figure 2.5 (d)) and the cycle repeats.

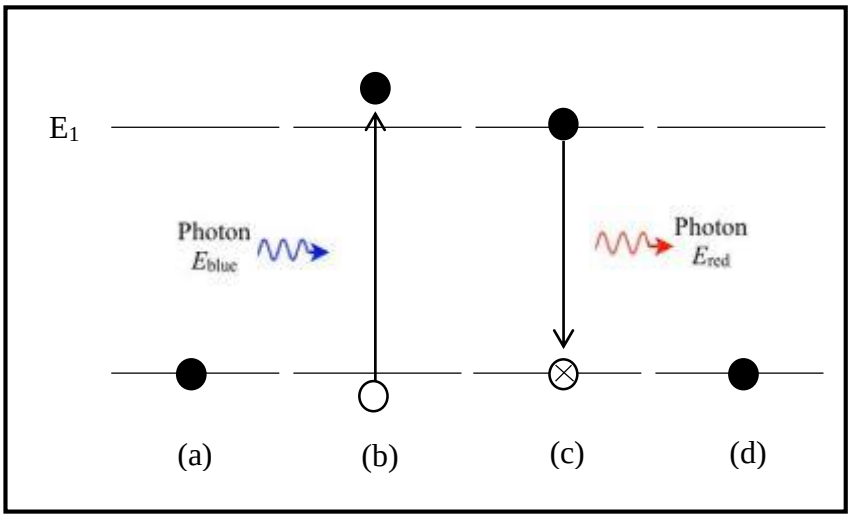

Figure 2.5. The steps of the photoluminescence process: (a) before absorption, (b) absorption, (c) radiative recombination. E_1 is the ground state for the electron, and the energy level at the bottom represents the ground state for holes.

Photoluminescence (PL) is the main characterization tool for studying the ZnO light emission process. The photoluminescence spectroscopy is a powerful tool to characterize ZnO optical processes and it provides valuable information for studying native defects and defect levels in materials. The PL emission spectra of ZnO consist of two major peaks which are near band edge (NBE) emission and deep-level emission (DLE) as shown in Figure 2.6 [22]. The NBE emission peak located at approximately 3.3 eV is dominated by free and bound exciton emission. The DLE emission band usually appears in the range of 1.7 eV to 2.4 eV depending on defect types or impurities.

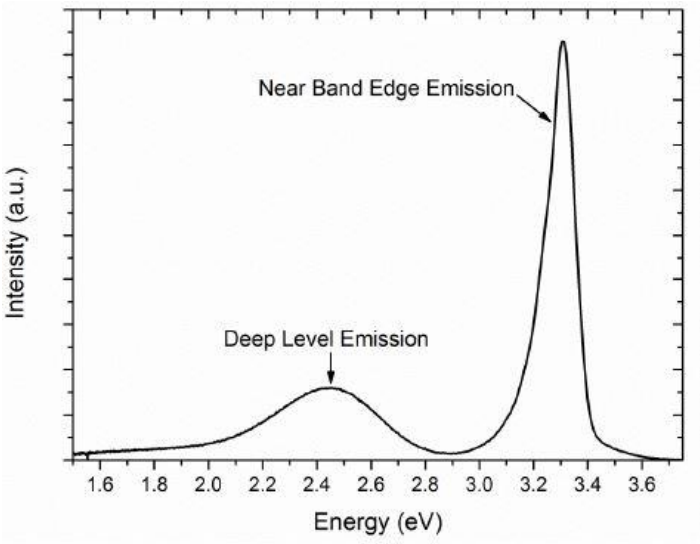

Figure 2.6 Characteristic ZnO luminescence spectrum presenting the near band edge (NBE) and the broad deep level emission (DLE) [22].

2.5.1 Defect Related to Deep Level Emission

Understanding the role of point defects in ZnO is an integral step in controlling the electrical and optical properties to develop next-generation devices. The defects can be introduced during the growth process or by post-growth treatments such as annealing or ion implantation. Native defects are imperfections in the crystal lattice that involve the constituent atoms only. Therefore, in ZnO, native point defects are only those involving Zn and/or O atoms. The point defects with deep levels in ZnO typically produce a broad luminescence band in the visible range located between 400 to 750 nm in the emission spectra. These deep level luminescence emissions are commonly observed as green, yellow as well as red luminescence [23]. The origin of these deep level emissions have considerable interest and is still under debate.

There are three common types of defects which are line defects, point defects and complex defects. Line defects belong to the rows of atoms such as dislocations,

while point defects belong to the isolated atoms in localized regions and the composition of more than one point defect forms the complex defects. There are intrinsic and extrinsic point defects and both contribute to the luminescence properties in ZnO. If the defects only consist of a host atom, then these defects are called intrinsic atoms. If foreign atoms such as impurities are involved in the defects then these defects are called extrinsic point defects. Intrinsic optical recombinations take place between the electrons in the conduction band and holes in the valance band. The deep level emission (DLE) band in ZnO has been previously attributed to different intrinsic defects in the crystal structure of ZnO such as oxygen vacancies (V_o), oxygen interstitial (O_i), zinc vacancies (V_{Zn}), zinc interstitial (Zn_i) and oxygen antisite (O_{Zn}) and zinc antisite (Zn_o).

The vacancy defects are formed when a host atom C is missing in the crystal and it is denoted by V_c. The most common vacancy defects in the ZnO are oxygen vacancy (V_O) and zinc vacancies (V_{Zn}). The single ionized oxygen vacancies in ZnO are responsible for the green emission in ZnO. While the double ionized oxygen vacancies are attributed to the red luminescence. The oxygen vacancy has lower formation energy than the zinc interstitial and dominates in zinc rich growth conditions. Many researchers also suggested oxygen vacancies as the source of green emission in ZnO [24]. Zinc vacancies were thoroughly investigated and suggested by many researchers to be the source of the green emission appeared at 2.4 - 2.6 eV below the conduction band in ZnO [25].

The interstitial defects are formed when an excess atom, D occupying an interstitial site between the normal sites in the crystal structure and it is denoted by D_i. The most common interstitial defects in the ZnO are oxygen interstitial (O_i) and

zinc interstitial (Zn_i). The zinc interstitial defects are normally located at 0.22 eV below the conduction band and play a vital role in the visible emissions in ZnO by recombination between Zn_i and different defects in the deep levels such as oxygen and zinc vacancies, oxygen interstitials and produce green, red and blue emissions in ZnO. Oxygen interstitials defects are normally located at 2.28 eV below the conduction band and are responsible for the orange-red emissions in ZnO [24].

The antisite defects are formed when atoms occupy the wrong lattice position. In ZnO, the oxygen and zinc antisite defects are formed when zinc occupies oxygen position or oxygen occupies a zinc position in the lattice. These defects can be introduced in ZnO by irradiation or ion implantation treatments. The transitions at 1.52 eV and 1.77 eV above the valance band are attributed to O_{Zn} related deep levels.

2.6 Theory of Random Laser

A laser is an optical device that emits light amplified by stimulated emission. Lasing requires two vital elements: gain material for stimulated emission to occur and an optical cavity to confine the light. When the total gain exceeds the losses, the system overcomes a threshold for lasing and emits laser emission. Random lasers on the other hand is not bounded by a cavity but relies on multiple scattering to confine the light.

Letokhov was first to discuss theoretically of the principle of random laser. He reported that amplification is scaled to the pump volume and the losses are proportional to the surface. When the gain exceeds the loss, light intensity increases